



Trade Science Inc.

April 2008

Volume 4 Issue 1

Macromolecules

An Indian Journal

Microreview

MMALJ, 4(1), 2008 [84-93]

Charge carrier mobility measurement in organic semiconductors

Sanjay Tiwari*², Shikha Tiwari¹

¹State Forensic Science Laboratory, Raipur, (CG) 492010, (INDIA)

²Cavendish Laboratory, University of Cambridge, Cambridge, CB3 0HE (U.K)

Tel : 0771-2263924; Fax : 0771-2263924

E-mail : st434@cam.ac.uk

Received: 19th October, 2007 ; Accepted: 24th October, 2007

ABSTRACT

Organic electronics and optoelectronics are newly emerging fields of science and technology that cover chemistry, physics, and materials science. Electronic and optoelectronic devices using organic materials are attractive because of the materials characteristics of light weight, potentially low cost, and capability of large-area, flexible device fabrication. Such devices as OLEDs, OPVs, and OFETs involve charge transport as a main process in their operation processes, and therefore, require high-performance charge-transporting materials. In this review article, first, some basic aspects of charge transport are discussed and then important mobility measurement techniques employed in electronic and optoelectronic devices such as OLEDs, OPVs, and OFETs are described.

© 2008 Trade Science Inc. - INDIA

KEYWORDS

Polymeric electronics;
Conjugated polymers;
Charge transport;
Mobility;
Polymeric field-effect transistor;
Polymeric light-emitting diode.

INTRODUCTION

Organic electronics has emerged as a vibrant field of research and development, spanning chemistry, physics, materials science, engineering, and technology^[1-3]. The rapid growth in the interest given to π -conjugated materials in general and organic semiconductors in particular is fueled by both academia and industry. On the basic research side, π -conjugated materials are fascinating systems in which a rich variety of new concepts have been uncovered due the interplay between their π -electronic structure and their geometric structure^[4-6]. On the applied research side, while not destined to replace silicon-based technologies, organic semiconductors promise the advent of fully flexible devices for large-area displays, solid-state lighting, radio frequency iden-

tification tags, or solar cells.

The devices mentioned above share a common trait: in all instances, their performance critically depends on the efficiency with which charge carriers (electrons and/or holes) move within the π -conjugated materials. The charge carriers are either injected into the organic semiconductors from metal or conducting oxide electrodes in the case of light-emitting diodes or field-effect transistors or generated within the materials in the case of solar cells via photon-induced charge separation at the interface between electron-donor and electron-acceptor components.

Since that first demonstration, organic thin films have proven useful in a number of applications, some of them now reaching the consumer market. The most successful is the organic light emitting device, or OLED, which

is currently used in long-lived and highly efficient color displays. Not far behind OLEDs are organic thin film transistors and low cost and efficient organic solar cells. Eventually, we may see more exotic devices such as organic lasers and memories.

Charge transport has been a subject of interest from the standpoints of both fundamental science and technology. Early studies of charge transport in organic materials were performed on both single crystals and disordered systems, for example, polymers and molecularly doped polymers, where small organic molecules are dispersed in a polymer binder. In particular, molecularly doped polymers have been studied extensively in view of their practical applications in photoreceptors in electrophotography. The recent development of small organic molecules that readily form stable amorphous glasses, namely, amorphous molecular materials, has enabled the studies of charge transport in the amorphous glassy state of small organic molecules without any binder polymers. Charge carrier mobilities of a number of organic polycrystals have also been determined from the performance of OFETs.

Mobility is one of the key parameters of interest both towards realizing improved device performance, as well as studying the underlying semiconductor physics in these materials. The measurement of low mobility ($\mu \ll 1 \text{ cm}^2 \text{ V}^{-1} \text{ s}^{-1}$) itself is an intriguing problem. Experimentally, the values of mobility obtained in polymeric FETs and LEDs show a difference of many orders of magnitude, whereas the mobility measurements by various photocarrier generation techniques present different transport scenarios. The unusual statistical mechanics of dispersive transport is also observed in these disordered systems. The mechanism of transport in semiconducting polymeric materials has been the source of much debate, and diverse models that attempt to explain it include carrier hopping between localized states, polaronic hopping and trapping/detrapping.

The ultimate goal of conducting polymer science is to produce materials and devices of higher quality. Towards this end, the study of charge transport phenomena in these materials is indispensable.

This review article focuses on charge-carrier mobility measurement techniques used in electronic and optoelectronic devices such as OLEDs, OPVs, and OFETs.

Characterization of charge mobility

The charge transport in conjugated polymers can involve many processes such as^[7]:

- (1) Conduction along the polymer backbone.
- (2) Hopping across chains due to inter-chain interactions.
- (3) Tunneling between conducting segments that are separated by less conducting regions, such as that observed in doped polymers like PA.

The charge carrier mobility (μ) in conjugated polymers is relevant to the operation of a wide range of electronic devices such as polymeric FETs (PFETs), polymeric LEDs (PLEDs), photoreceptors and photovoltaics. For example, the current through a PLED or the power of a solar cell are governed by mobility. The mobility in inorganic semiconductors, defined as the ratio of average carrier drift velocity (v_d) to the applied electric field (E), assumes large values ($\mu \gg 1 \text{ cm}^2 \text{ V}^{-1} \text{ s}^{-1}$) on account of the nature of charge transport (largely due to diffusion in bands) in these materials. The charge carriers (electrons/holes) in inorganic semiconductors move as highly delocalized plane waves in broad bands, and their motion is limited by scattering from acoustic phonons (lattice vibrations) or by charged defects (ionized donors or acceptors). The scattering of carriers is reflected in the temperature dependence of the mobility ($\mu \propto T^{-3/2}$ for phonon scattering)- therefore the mobility increases as the temperature decreases.

In a disordered system, like semiconducting polymers, transport involves phenomena such as hopping

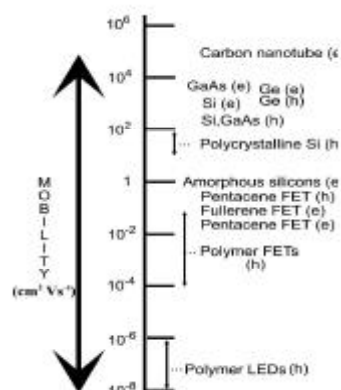


Figure 1: Mobility of semiconducting polymers compared with that of other semiconductors. Here 'e' denotes electron mobility and 'h' is the hole mobility

Microreview

between localized sites wherein the phonons help overcomes the energy difference between sites. The mobility due to thermally assisted hopping is many orders of magnitude lower than that due to band transport; however, the mobility is increased upon increasing the temperature. The mobility of conjugated polymers is compared with other semiconducting materials in figure 1.

As we know when a voltage is applied to a sample sandwiched between two electrodes, charge carriers, that is, holes and electrons are transported across the sample under the electric field. The main concerns with charge transport are how fast and by what mechanism charge carriers are transported.

The velocity of charge carriers is proportional to the strength of the applied electric field and is expressed as eq

$$v = \mu F \quad (1)$$

where v is the velocity of charge carriers, F is the strength of electric field, and the proportional constant μ is the drift mobility of charge carriers, that is, the distance over which charge carriers are transported per second under the unit electric field. It should be noted that μ is dependent upon the electric field for organic disordered systems.

The charge carrier mobilities of organic materials greatly vary depending on the kind of charge carriers, namely, whether they are holes or electrons, molecular structures, and materials morphologies. Different transport mechanisms are operative depending on the aggregation states of materials, for example, crystalline and amorphous states.

Experimental measurements of carrier mobilities

The large mobility in inorganic semiconductors is determined by the Hall effect and conductivity measurements^[8] The drift mobility is then related to the Hall mobility by a scattering factor that depends upon the scattering mechanisms and distribution function of carriers. This technique is not suitable for high-resistance, low-mobility polymers; hence other approaches have been used (Figure 2).

The charge carrier drift mobility has been determined by various techniques, some of which are time-of-flight (TOF) method^[9-10]; analysis of steady-state, trap-free, space-charge limited current (steady-state TF-SCLC method)^[9,11]; analysis of dark injection space-

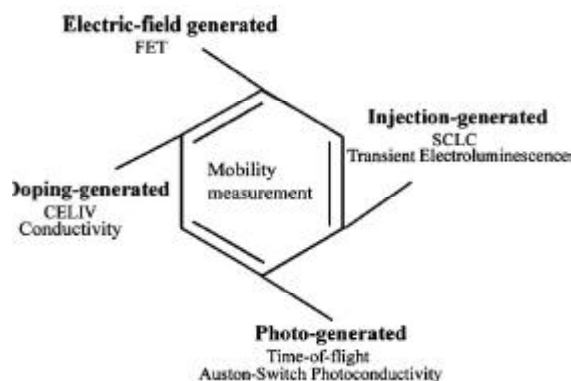


Figure 2: Various types of mobility measurements

charge-limited transient current (DI-SCLC method)^[9]; analysis of the performance of OFETs (FET method)^[12]; measurement of transient electroluminescence (EL) by the application of step voltage (transient EL method)^[13-16]; and pulse radiolysis time-resolved microwave conductivity (PR-TRMC) technique^[17]. Results from methods that measure mobilities over macroscopic distances (~1 mm) are often dependent on the purity and order in the material. Methods that measure mobilities over microscopic distances are less dependent on these characteristics. We briefly describe below the basic principles of some of the most widely referenced methods.

Time-of-flight (TOF) method

TOF measurements have been studied most extensively with organic disordered systems such as polymers and molecularly-doped polymers in where low molecular-weight organic materials are dispersed in binder polymers. The TOF method is based on the measurement of the carrier transit time ($\hat{\delta}$), namely, the time required for a sheet of charge carriers photogenerated near one of the electrodes by pulsed light irradiation to drift across the sample to the other electrode under an applied electric field.

Samples used for the measurement are either a single charge-transporting layer or double layers consisting of charge carrier generation and transport layers (CGL and CTL, respectively) sandwiched between the two electrodes, one of which is transparent. In the case of measuring a hole drift mobility, the transparent electrode is held at a positive potential with respect to the ground, while the other one is grounded through a resistance R which has a much smaller resistance than the

sample. This leads to an applied potential V in the material. Hole charges are generated by photo-excitation of the film through irradiation with a short pulse laser (the wavelength of which depends on the absorption band of materials). One of the advantages of using TOF technique is that the hole and electron mobility can be studied separately. Photo-generated charge carriers will start moving to the negative electrode. The drifting carriers build a current equal to Nev/d ; where N is the number of charge carriers in the material, e is the elementary charge, d is the film thickness, and v is the velocity. For current measurements, the condition $CR \ll \hat{\delta}$ (C the total capacitance across resistance R) is necessary to prevent the rising time of the signal from being longer than the transit time $\hat{\delta}$. The transit time ($\hat{\delta}$) is defined as the time the band of charge carriers needs to travel through the sample

The thickness of samples is usually in the range from 5 to 20 μm . The samples are prepared using vacuum evaporation, solvent cast from solution, or by pressing melt samples with two ITO electrodes. In the case of the double layer structure (Figure 3), irradiated pulsed light is transmitted through the transparent CTL and absorbed by the CGL. Copper phthalocyanine and perylenebis(dicarboximide)s can be used as CGL materials. One of the charge carriers, either holes or electrons, photogenerated in the CGL is injected into the CTL and then drifts across the CTL to the electrode. Alternatively, photogeneration of charge carriers takes place at the interface between the CGL and CTL depending upon the kind of CGL materials. When charge carriers start to drift, photocurrents flow until the charge carriers arrive at the other electrode. Figure 4 shows a typical transient experimentally determined from the cusp of nondispersive photocurrent, as shown in the figure. In contrast to the non-dispersive photocurrent in

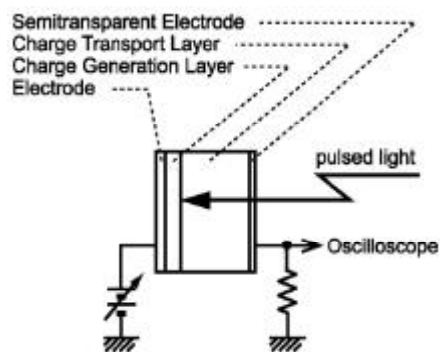


Figure 3: Schematic diagram of apparatus for a time-of-flight method

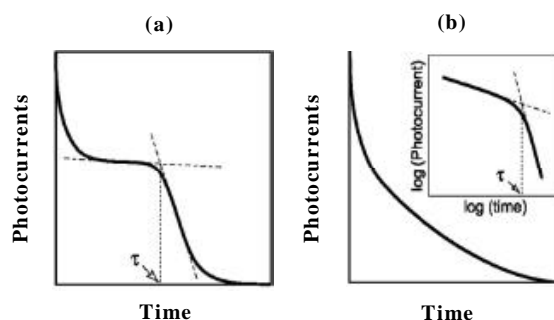


Figure 4 : Typical transient photocurrents: (a) nondispersive; (b) dispersive. Inset: double logarithmic plot

Figure 4a, the transient photocurrents observed for polymers and molecularly doped polymers are often dispersive without any definite cusp as shown in figure 4b. In this case, $\hat{\delta}$ is determined from the double logarithmic plots of transient photocurrents, according to the Scher-Montroll theory^[18].

The theoretical transient current as a function of time is shown in figure 5a. At the excitation of one side of the material, the transient current (j_{ph} =photo-generated current density) increases instantly. In the following time, the photo-generated carriers are traveling through the material, and the current level should stay constant. As soon as the carriers reach the other electrode, the cur-

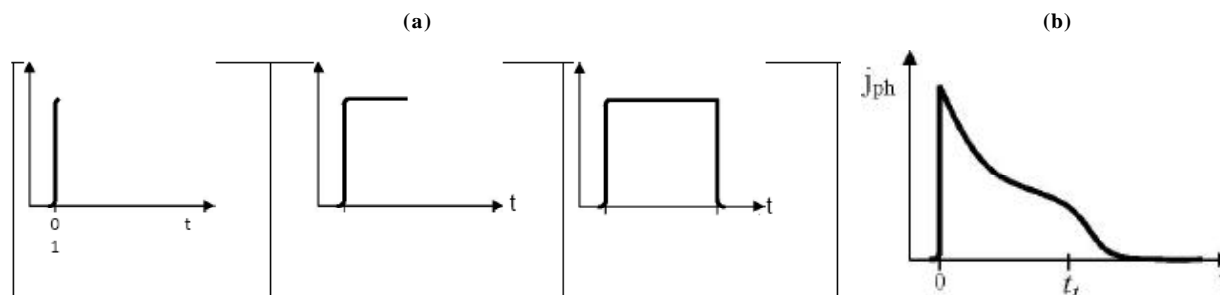


Figure 5: Pulse shape in case of deep traps conditions

Microreview

rent will decrease rapidly, thus makes a signal. In order to obtain a sufficient transient signal to allow evaluate a transient time, the photo-generated charge carriers have not to be dispersed. Therefore it is important that the duration of the excitation pulse is much shorter than the transient time t_t , and the absorption depth of the excitation is smaller than the thickness of the sample. However, many organic materials under study in TOF experiments with a proper condition could not obtain an ideal transient sharp due to deep traps in materials. Typical signal of an amorphous organic material is shown in figure 5b. This sharp is due to a charge trap or dispersion effect in a material, which means that some charge carriers are hold in different energy levels from a transporting level for a certain time during traveling from one electrode to the other. Such a transient sharp has to be examined in double logarithmic current versus time plot. In this case, the transient time is determined as the intersection between two straight lines with different slopes at short and long times of the transient photocurrent

The transit time ($\hat{\delta}$) is given by eq 2, where v is the velocity of charge carriers and d is the sample thickness. When eqs 1 and 2 are combined, the charge carrier drift mobility (μ) is expressed as eq 3.

$$\tau = d/v \quad (2)$$

$$\mu = d^2/V\tau \quad (3)$$

In TOF experiments, relatively thick samples of a few to several micrometers are favorable due to the requirement of a smaller absorption depth of the excitation relative to the film thickness. In addition, determining mobilities for materials having a high charge carrier density is difficult because diffusive charge carriers will affect the drift of photogenerated charge carriers under an electric field.

TF-SCLC method

The measurement of carrier drift mobility by the steady state TF-SCLC method is based on the analysis of current density (J)-applied voltage (V) characteristics in the dark. Generally, the J - V characteristics are linear at low drive voltages, showing ohmic behavior. At high applied voltages, the J - V characteristics become space-charge-limited because of the injection of charge carriers from one electrode. When the contact between the electrode and the organic layer is ohmic

and the current is transport-limited instead of injection limited, the space-charge-limited current J is given by eq 4, which is known as the Mott-Gurney equation^[9],

$$J = \frac{9}{8} \epsilon \mu \frac{V^2}{d^3} \theta = \frac{9}{8} \epsilon \mu \frac{1}{d} F^2 \theta \quad (4)$$

where ϵ and d are the permittivity and thickness of the sample, and θ is a factor that considers the presence of charge carrier traps, that is, the ratio of the number of free carriers to the total number of carriers. When the current flow is in agreement with SCLC, J should be proportional to the square of the electric field (F^2), which is dependent upon the sample thickness. When θ is equal to 1, the current becomes trap free SCLC. The charge carrier mobility can be evaluated from this equation on the basis of the assumption that the contact between the electrode and the organic layer is ohmic without any energy barrier for charge injection. In case the mobility data determined by other methods are available, one can calculate J . When the experimental value of J is equal to the calculated value, the contact between the organic layer and the electrode is regarded to be an ideal ohmic one. Equation 4 applies for materials in which the mobility is independent of the electric field. Since the charge carrier mobility of organic disordered systems is usually electric field dependent, in agreement with the Poole-Frenkel effect, eq 4 is modified as eq 5^[19],

$$J = \frac{9}{8} \epsilon \mu_0 \exp(\beta F^{1/2}) \frac{1}{d} F^2 \theta \quad (5)$$

where μ_0 is the mobility when $F=0$. If the mobility is independent of the electric field, $\beta=0$

In the DI-SCLC method, a step voltage is applied to the sample sandwiched between two electrodes, one

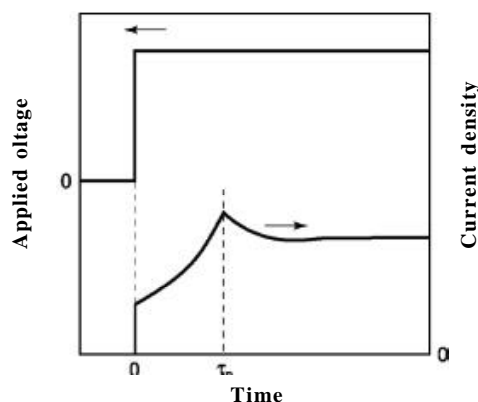


Figure 6: Typical DI-SCLC

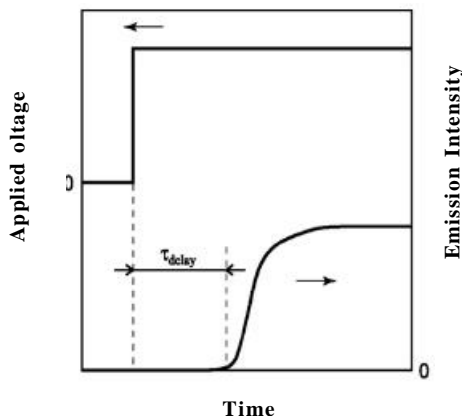


Figure 7 : Typical transient emission behavior of OLEDs

of which forms an ohmic contact. An ideal transient current for trap free materials is shown in figure 6. The current increases with time, reach the maximum at time $\hat{0} p$, and then gradually decrease to a constant current, which is steady state SCLC. $\hat{0} p$ is related to space-charge-free transit time $\hat{0} \delta$ as expressed by eq 6, and the mobility can be calculated from eq 7.

$$\tau_p \sim 0.786 \tau_0 \quad (6)$$

$$\mu = D^2 / V \tau_0 \sim 0.786 \times D^2 / V \tau_p \quad (7)$$

The transient EL method is based on the measurement of a time delay between the application of a step voltage and the onset of emission, as shown in figure 7. The onset of emission is determined by the arrival of the slower charge carrier of the injected carriers at the emission zone.

Auston switch technique

A micro-stripline Auston switch-based picoseconds photoconductivity technique has also been used in place of TOF. Measurements in a-Se and PPV suggest possible new implications such as two distinct transport mechanisms^[20-21]:

- (1) a short-lived transport involving carrier dynamics in extended band states until the carrier progressively tunnels into lower states, involving a different mobility; and
- (2) a long-lived transport in multiple-trapping band tails with low mobility.
- (3) It was also suggested that a built-in potential barrier at metal–semiconductor interfaces influences the shape of photocurrent in TOF experiments

Field-effect transistor mobility

The carrier mobilities can be extracted from the electrical characteristics measured in a field-effect transistor (FET) configuration. The I-V (current-voltage) expressions derived for inorganic-based transistors in the linear and saturated regimes prove to be readily applicable to organic transistors (OFETs)^[22]. These expressions read in the linear regime:

$$I_{SD} = \frac{W}{L} \mu C (V_G - V_T) V_{SD} \quad (5)$$

and in the saturated regime:

$$I_{SD} = \frac{W}{2L} \mu C (V_G - V_T)^2 \quad (6)$$

Here, I_{SD} and V_{SD} are the current and voltage bias between source and drain, respectively, V_G denotes the gate voltage, V_T is the threshold voltage at which the current starts to rise, C is the capacitance of the gate dielectric, and W and L are the width and length of the conducting channel. In FETs, the charges migrate within a very narrow channel (at most a few nanometers wide) at the interface between the organic semiconductor and the dielectric^[23-24].

Transport is affected by structural defects within the organic layer at the interface, the surface topology and polarity of the dielectric, and/or the presence of traps at the interface (that depends on the chemical structure of the gate dielectric surface). Also, contact resistance at the source and drain metal/organic interfaces plays an important role; the contact resistance becomes increasingly important when the length of the channel is reduced and the transistor operates at low fields; its effect can be accounted for via four-probe measurements^[25-27].

The charge mobilities extracted from the OFET I-V curves are generally higher in the saturated regime than those in the linear regime as a result of different electric-field distributions. The mobility can sometimes be found to be gate-voltage dependent^[28]; this observation is often related to the presence of traps due to structural defects and/or impurities (that the charges injected first have to fill prior to establishment of a current) and/or to dependence of the mobility on charge carrier density (which is modulated by V_G)^[29].

The dielectric constant of the gate insulator also affects the mobility; for example, measurements on rubrene single crystals^[30] and polytriarylamine chains^[31] have shown that the carrier mobility decreases with increas-

Microreview

ing dielectric constant due to polarization (electrostatic) effects across the interface; the polarization induced at the dielectric surface by the charge carriers within the organic semiconductor conducting channel, couples to the carrier motion, which can then be cast in the form of a Frölich polaron^[32-35].

Diode method

The mobilities can also be obtained from the electrical characteristics of diodes built by sandwiching an organic layer between two electrodes (provided that transport is bulk limited and not contact limited). The choice of the electrodes is generally made in such a way that only electrons or holes are injected at low voltage. In the absence of traps and at low electric fields, the current density J scales quadratically with applied bias V . Such behavior is characteristic of a space-charge limited current (SCLC); it corresponds to the current obtained when the number of injected charges reaches a maximum because their electrostatic potential prevents the injection of additional charges^[36]. In that instance, the charge density is not uniform across the material and is largest close to the injecting electrode^[37]. In this regime, when neglecting diffusion contributions, the J - V characteristics can be expressed as

$$J = \frac{9}{8} \epsilon_0 \epsilon_r \mu \frac{V^2}{L^3} \quad (7)$$

where ϵ_r denotes the dielectric constant of the medium and L is the device thickness. Note that a field-dependence of the mobility has to be considered at high electric fields (vide infra).

The J - V curves become more complex in the presence of traps. They first exhibit a linear regime, where transport is injection-limited, followed by a sudden increase for an intermediate range of applied biases; finally, the V^2 dependence of the trap-free SCLC regime is reached. The extent of the intermediate region is governed by the spatial and energetic distribution of trap states, which is generally modeled by a Gaussian^[38] or exponential distribution^[39].

Pulse-radiolysis time-resolved microwave conductivity (pr-trmc)

Here, the sample is first excited by a pulse of highly energetic electrons (in the MeV range) to create a low density of free carriers. The change in electrical con-

ductivity $\Delta\sigma$ induced by the pulse is then measured via the change in microwave power reflected by the sample and is therefore frequency dependent. $\Delta\sigma$ can be expressed as^[40]

$$\Delta\sigma = e \sum \mu N_{e-h} \quad (8)$$

where $\sum\mu$ is the sum of hole and electron mobilities and N_{e-h} is the density of generated electron-hole pairs. N_{e-h} is estimated by dividing the amount of energy density transferred to the material by the energy required to create one electron-hole pair; this ratio is further multiplied by a survival probability that accounts for possible charge-recombination mechanisms during the duration of the pulse. With this technique, the charges are directly generated in the bulk; their transport properties are probed on a very local spatial scale (for instance, along a portion of a single polymer chain) determined by the frequency of the microwave radiations (the lower the frequency, the larger the region that is explored); the charges trapped by impurities or structural defects are not responsive. PR-TRMC is a contact-free technique that is not affected by space-charge effects and can be applied to bulk materials as well as to single polymer chains in solution.

Because of its local character, PR-TRMC is considered to provide intrinsic AC mobility values for the bulk; these values should be seen as upper limits for the mobilities at low fields. TOF values are generally smaller since such DC measurements probe a macroscopic range and force the charge carriers to cross structural defects and to interact with impurities. The AC and DC mobility values generally deviate above a threshold frequency that depends on the degree of order in the samples. However, there are instances in which the two techniques result in similar mobility values, for example, in the case of discotic liquid crystals based on hexathiohexyl triphenylenes, materials that have been used as reference compounds to validate the PR-TRMC technique^[41]. PR-TRMC experiments on polythiylenevinylene^[42] and polyparaphenylenevinylene^[43] chains provide hole[electron] mobility values of 0.38[0.23] and 0.06[0.15] cm²/V·s, respectively (here, one kind of charge carriers was alternatively selectively trapped to determine the individual mobilities). A mobility as high as 600 cm²/V·s has been recently inferred from measurements in dilute solution along fully planar,

ladder-type polyparaphenylene chains^[44] this result confirms that the elimination of torsional degrees of freedom along polymer chains is a key step to increase charge mobilities. In polymer films, charge mobilities are expected to be limited by interchain transport; to reach mobilities over $0.1 \text{ cm}^2/\text{V}\cdot\text{s}$ requires a high degree of interchain structural order.

CELIV technique

A charge extraction by linearly increasing voltage (CELIV) technique has also been applied recently for mobility estimation in RR-P3HT^[45]. A linearly increasing electric field is applied at one electrode and the current transient is used to obtain the value of mobility that arises from 'doping-induced' charged carriers. The temperature and electric field dependence of mobility obtained from TOF agrees well with CELIV mobility indicating that the mode of carrier generation (i.e. photo-generation versus doping-induced) has no significant effect.

Photo-induced transient stark spectroscopy

This technique, recently described, involves an electrode-less method for obtaining the intrinsic mobility, i.e. mobility not limited by traps and defects in the material or by recombination^[46]. The ground state electroabsorption is studied during charge separation when photo-induced electron-hole pairs are generated. When these carriers drift apart, (i.e. photo-induced polarization takes place) their dipole nature opposes the electric field, thus leading to a change in the measured Stark effect. The intrinsic charge carrier mobility and electron-hole separation can be inferred from this experiment in the picoseconds regime^[46]. Similar to the results presented by the Auston switch technique (see above), this experiment has also suggested large intrinsic mobility before the transition to slower transport takes place, due to trapping and recombination in the nanosecond time scale.

Comparisons of Mobilities Measured by Different Methods

One of the important differences between the different mobility measurement methods is the geometry of the sample in which the charge mobility is characterized. The thickness of samples for the measurement is different depending upon the method. In TOF and

SCLC, the sample is sandwiched between two electrodes and the conduction of the charges is perpendicular to the substrate plane. By contrast, in a FET the charge mobility is characterized within the plane of the substrate.

This geometrical difference is irrelevant when one study the charge transport properties in an amorphous material but becomes fundamental when the material present some molecular organization such as liquid crystal materials or crystalline materials. The question is whether these different methods give almost the same mobility values. It has been reported that mobility values are different depending on the thickness of samples especially for low-mobility dispersive materials^[47-49]. Comparative studies of charge transport using different techniques have been made for certain classes of materials, for example, m-MTDATA^[50-52] OMeTAD^[53], R-NPD^[51,54], Alq3^[55], CuPc^[56], and so forth. The hole mobilities of m-MTDATA and R-NPD determined by the DI-SCLC method have been shown to be in excellent agreement with those determined by the TOF method^[51]. Room-temperature mobilities of OMeTAD (**142**) measured by three independent methods, TOF, DI-SCLC, and steady-state TF-SCLC methods, have been shown to agree well over a range of sample thicknesses from 4nm to 135 nm^[53]. The plots of the logarithm of electron mobilities of Alq3 measured by the transient EL and TOF methods as a function of the square root of the electric field have been shown to be on the same line, and hence, the results measured by the two methods are in good agreement with each other^[55]. Comparison of the hole mobility data of CuPc by the TOF and FET methods shows that they gave almost the same results; iFET) $(0.94-1.3)\cdot 10^{-3} \text{ cm}^2 \text{ V}^{-1} \text{ s}^{-1}$ and (TOF) $(1.5-2.0)\cdot 10^{-3} \text{ cm}^2 \text{ V}^{-1} \text{ s}^{-1}$ ^[56]. Likewise, mobility data for m-MTDATA determined by the TOF and FET methods were almost the same^[52]. On the other hand, iFET values of TPTPA(**81**), TTB (**315**), TPD, and R-NPD were approximately 2 orders of magnitude smaller than those determined by the TOF method^[52, 54].

CONCLUSIONS

A significant progress has been made on charge transport in amorphous molecular materials, but the re-

Microreview

relationship between molecular structures and charge carrier drift mobilities remains to be investigated. The materials which have been put to practical applications are few in number. The ultimate goal of conducting polymer science is to produce materials and devices of higher quality. Towards this end, the study of charge transport phenomena and mobility in these materials is indispensable. In the review, different techniques used for mobility measurement has been discussed in detail and comparison of mobilities measured by different techniques are described.

A future progress will be directed toward a deeper understanding of materials chemistry and device physics, development of new devices including memories and sensors, fabrication of flexible devices, and integration of multifunctions in a single device.

ACKNOWLEDGMENT

The first author (ST) acknowledges the financial support from British Council under UKIERI program

REFERENCES

- [1] S.R.Forrest; *Chem.Rev.*, **97**, 1793 (1997).
- [2] L.S.Hung, C.H.Chen; *Mater.Sci.Eng.*, **39**, 143 (2002).
- [3] D.Berner, H.Houili, W.Leo, L.Zuppiroli; *Phys.Status Solidi.*, **A202**, 9 (2005).
- [4] W.P.Su, J.R.Schrieffer, A.J.Heeger; *Phys.Rev.Lett.*, **42**, 1698 (1979).
- [5] J.L.Bredas, G.B.Street; *Acc.Chem.Res.*, **18**, 309 (1985).
- [6] A.J.Heeger, S.Kivelson, J.R.Schrieffer, W.P.Su; *Rev.Mod.Phys.*, **60**, 781 (1988).
- [7] K.Ehinger, S.Roth; 'Electronic Properties of Polymers and Related Compounds', H.Kuzmany, M.Mehring, S.Roth (Eds.); Springer Verlag, Berlin (1985).
- [8] C.Hamaguchi; *Basic Semiconductor Physics*, Springer, New Delhi, 263 (2001).
- [9] M.A.Lampert, P.Mark; 'Current Injection in Solids', Academic Press: New York, (1970).
- [10] J.Mort, D.M.Pai; Eds *Photoconductivity and Related Phenomena*, Elsevier, New York, (1976).
- [11] Z.An, J.Yu, S.C.Jones, S.Barlow, S.Yoo, B.Domercq, P.Prins, L.D.A.Siebbeles, B.Kippelen, S.R.Marder; *Adv.Mater.*, **17**, 2580 (2005).
- [12] S.M.Sze; 'Physics of Semiconductor Devices', 2nd ed., Wiley, New York, (1981).
- [13] C.Hosokawa, H.Tokailin, H.Higashi, T.Kusumoto; *Appl.Phys.Lett.*, **60**, 1220 (1992).
- [14] C.Hosokawa, H.Tokailin, H.Higashi, T.Kusumoto; *Appl.Phys.Lett.*, **63**, 1322 (1993).
- [15] M.Redecker, H.Bassler, H.H.Horhold; *J.Phys.Chem.B.*, **101**, 7398 (1997).
- [16] T.C.Wong, J.Kovac, C.S.Lee, L.S.Hung, S.T.Lee; *Chem.Phys.Lett.*, 334, 61 (2001).
- [17] P.G.Schouten, J.M.Warman, M.P.de Haas; *J.Phys.Chem.*, **97**, 9863 (1993).
- [18] H.Scher, E.W.Montroll; *Phys.Rev.B*, **12**, 2455 (1975).
- [19] P.N.Murgatroyd; *J.Phys.D*, **3**, 151 (1971).
- [20] D.Moses; *Phys.Rev.B.*, **53**, 4462 (1996).
- [21] D.Moses; *Solid.State.Commun.*, **69**, 721 (1989).
- [22] G.Horowitz; *Adv.Mater.*, **10**, 365 (1998).
- [23] G.Horowitz; *J.Mater.Res.*, **19**, 1946 (2004).
- [24] A.Dodabalapur; L.Torsi, H.E.Katz; *Science*, **268**, 270 (1995).
- [25] P.V.Pesavento, R.J.Chesterfield, C.R.Newman, C.D.Frisbie; *J.Appl.Phys.*, **96**, 7312 (2004).
- [26] C.Goldmann, S.Haas, C.Krellner, K.P.Pernstich, D.J.Gundlach, B.Batlogg; *J.Appl.Phys.*, **96**, 2080 (2004).
- [27] V.Podzorov, S.E.Sysoev, E.Loginova, V.M.Pudalov, M.E.Gershenson, *Appl.Phys.Lett.*, **83**, 3504 (2003).
- [28] C.D.Dimitrakopoulos, S.Purushothaman, J.Kymissis, A.Callegari, J.M.Shaw; *Science*, **283**, 822 (1999).
- [29] C.Tanase, E.J.Meijer, P.W.M.Blom, D.M.de Leeuw; *Phys.Rev.Lett.*, **91**, 216601 (2003).
- [30] A.F.Stassen, R.W.I.de Boer, N.N.Iosad, A.F.Morpurgo; *Appl.Phys.Lett.*, **85**, 3899 (2004).
- [31] J.Veress, S.D.Ogier, S.W.Leeming, D.C.Cupertino, S.M.Khaffaf; *Adv.Funct.Mater.*, **13**, 199 (2003).
- [32] N.Kirova, M.N.Bussac; *Phys.Rev.B*, **68**, 235312 (2003).
- [33] H.Houili, J.D. Picon, L.Zuppiroli, M.N.Bussac; *J.Appl.Phys.*, **100**, 023702 (2006).
- [34] I.N.Hulea, S.Fratini, H.Xie, C.L.Mulder, N.N.Iosad, G.Rastelli, S.Ciuchi, A.F.Morpurgo; *Nat. Mater.*, **5**, 982 (2006).
- [35] V.Coropceanu, J.L.Bredas; *Nat.Mater.*, **5**, 929 (2006).
- [36] P.W.M.Blom, M.J.M.deJong, J.J.M.Vleggaar; *Appl. Phys.Lett.*, **68**, 3308 (1996).
- [37] D.Fichou; 'Handbook of Oligo- and Polythiophenes', Wiley-VCH, Weinheim, New York, (1999).

Microreview

- [38] H.Bassler; Phys.Status Solidi B., **175**, 15 (1993).
- [39] G.Horowitz, M.E.Hajlaoui, R.Hajlaoui; J.Appl. Phys., **87**, 4456 (2000).
- [40] A.M.Van de Craats, J.M.Warman; Adv.Mater., **13**, 130 (2001).
- [41] J.M.Warman, M.P.de Haas, G.Dicker, F.C.Grozema, J.Piris, M.G.Debije; Chem.Mater., **16**, 4600 (2004).
- [42] P.Prins, L.P.Candeias, A.J.M.Van Breemen, J.Sweelssen, P.T.Herwig, H.F.M.Schoo, L.D.A.Siebbeles; Adv.Mater., **17**, 718 (2005).
- [43] R.J.O.M.Hoofman, M.P.de Haas, L.D.A.Siebbeles, J.M.Warman; Nature, **392**, 54 (1998).
- [44] P.Prins, F.C.Grozema, J.M.Schins, T.J.Savenije, S.Patil, U.Scherf, L.D.A.Siebbeles; Phys.Rev.B, **73**, 045204 (2006).
- [45] A.J.Mozer, N.S.Sariciftci, A.O.Pivrikas, R.Sterbacka, G.Jusuka, L.Brassat; Phys.Rev.B, **71**, 035214 (2005).
- [46] J.Cabanillas-Gonzalez, T.Virgili, A.Gambetta, G.Lanzani, T.D.Anthopoulos, D.M.de Leeuw; Phys. Rev.Lett., **96**, 106601 (2006).
- [47] D.Poplavskyy, J.Nelson; J.Appl.Phys., **93**, 341 (2003).
- [48] P.M.Borsenberger, L.T.Pautmeier, H.Bassler; Phys. Rev.B, **46**, 12145 (1992).
- [49] K.Okumoto, K.Wayaku, T.Noda, H.Kageyama, Y. Shirota; Synth.Met., **111-112**, 473 (2000).
- [50] C.Giebeler, H.Antoniadis, D.D.C.Bradley, Y.Shirota; Appl.Phys.Lett., **72**, 2448 (1998).
- [51] S.C.Tse, S.W.Tsang, S.K.So; J.Appl.Phys., **100**, 063708 (2006).
- [52] Y.Shirota, K.Okumoto, H.Ohishi, M.Tanaka, M.Nakao, K.Wayaku, S.Nomura, H.Kageyama; Proc.SPIE-Int.Soc.Opt.Eng., **5937**, 593717 (2005).
- [53] M.Kimura, S.Inoue, K.Shimada, S.Tokito, K.Noda, Y.Tagu, Y.Sawaki; Chem.Lett., **192**, (2000).
- [54] T.P.I.Saragi, T.Fuhrmann-Lieker, J.Salbeck; Adv.Funct.Mater., **16**, 966 (2006).
- [55] S.C.Tse, H.H.Fong, S.K.So; J.Appl.Phys., **94**, 2033 (2003).
- [56] M.Kitamura, T.Imada, S.Kako, Y.Arakawa; Jpn.J. Appl.Phys., **43**, 2326 (2004) .